Proc. Natl. Acad. Sci. USA
Vol. 87, pp. 988–992, February 1990
Neurobiology

Synchronous neural networks of nonlinear threshold elements with hysteresis

(bistability/noise/action potentials/associative memory/pattern recognition)

LIPO WANG AND JOHN ROSS*

Department of Chemistry, Stanford University, Stanford, CA 94305

Contributed by John Ross, October 19, 1989

ABSTRACT **We use Hoffmann's suggestion [Hoffmann, G. W. (1986) *J. Theor. Biol.* 122, 33–67] of hysteresis in a single neuron level and determine its consequences in a synchronous network made of such neurons. We show that the overall retrieval ability in the presence of noise and the memory capacity of the network in the present model are better than in conventional models without such hysteresis. Second-order interaction further improves the retrieval ability of the network and causes hysteresis in the retrieval-noise curve for any arbitrary width of the bistable region. The convergence rate is increased by the hysteresis at high noise levels but is reduced by the hysteresis at low noise levels. Explicit formulae are given for calculations of average final convergence and noise threshold as functions of the width of the bistable region. There is neurophysiological evidence for hysteresis in single neurons, and we propose optical implementations of the present model by using ZnSe interference filters to test the predictions of the theory.**

Neural networks (1–21) have become the focus of considerable research effort recently (for recent reviews on neural networks, see refs. 1–3). These seemingly simple systems show intriguing properties such as learning, memory, and fault-tolerant information retrieval. Two key features of a neural network model are (*i*) the properties of each individual neuron and (*ii*) the connectivity between neurons. Variations in either the properties of a single neuron or synaptic correlations among neurons are expected to alter the emergent characteristics of the neural network.

In the present paper, we consider theoretically a feature new to conventional synchronous neural networks of associative memory—that is, nonlinear threshold elements with hysteresis. The existence of hysteresis at the level of a single neuron has been recently proposed by Hoffmann (18) in a neural network model based on the analogy with the immune system. The purpose of our present paper is to adopt and apply Hoffmann's suggestion of hysteresis at a single neuron level and determine its consequences in a synchronous neural network. We show that the retrieval property in the presence of noise and the memory capacity of the network in the present model are better than that of conventional synchronous models, where it has been assumed that there is no such hysteresis. Inclusion of higher-order interaction further improves these advantages. We seek and find some experimental neurophysiological evidence for hysteresis in the response of a single neuron. We also discuss possible implementations of the present model.

BASIC FORMULATION

We consider N threshold elements that have two states—i.e., $S_i = \pm 1$—which is the same as the McColluch–Pitts neurons (22) in conventional neural network models of associative memory (4–6). The dynamics in the present model is different, however; the input–output response functions for both the conventional and the present model are given in Figs. 1 and 2, respectively. In the conventional model, hysteresis does not exist in the neuronal response function (see Fig. 1). For simplicity, we focus on the discrete case shown by Fig. 2*A*, and we consider a synchronous updating algorithm (4, 8, 20, 21).

Suppose that

$$h_i(t) = \sum_{j=1}^{N} T_{ij} S_j(t) + \eta_i \qquad [1]$$

is the total input signal for the ith neuron, where $S_j(t)$ represents the state of the jth neuron at time t,

$$T_{ij} = \frac{1}{N} \sum_{\mu=1}^{p} S_i^{\mu} S_j^{\mu}, \qquad [2]$$

with $T_{ii} = 0$, is the synaptic efficacy according to the Hebbian rule (7, 23), $\vec{S}^{\mu}$ is the μth stored pattern, and p is the number of patterns stored. We include in Eq. 1 a random Gaussian noise η_i with a SD σ_o to take into account the presence of noise. Neural noise in physiological systems has largely been attributed to spontaneous neural firing and the statistical variation in the number of vesicles containing neurotransmitters, such as acetylcholine, released at the synaptic junctions (24–27). (For experimental evidence that supports a *Gaussian* noise distribution, see, for example, ref. 26, p. 21.) In artificial implementations of neural networks (11–17), noise may result from electrical, thermal, and quantum fluctuations. The updating rule in the present model is as follows (see Fig. 2*A*):

$$S_i(t+1) = \begin{cases} +1 \text{ if } S_i(t) = +1 \text{ and } h_i(t) > -\alpha; \\ -1 \text{ if } S_i(t) = +1 \text{ and } h_i(t) < -\alpha; \\ \qquad \text{or } S_i(t) = -1 \text{ and } h_i(t) > \alpha \\ \qquad \text{or } S_i(t) = -1 \text{ and } h_i(t) < \alpha \end{cases}, \qquad [3]$$

where α is the half-width of the bistable region. Eq. 3 can be cast into the following compact form:

$$S_i(t+1) = \text{sign}[h_i(t) + \alpha S_i(t)]. \qquad [4]$$

where $\text{sign}(x) = -1$ for negative x and $\text{sign}(x) = +1$ for positive x.

Suppose that the initial state of the network is set in the neighborhood of pattern $\vec{S}^1$. Explicitly, we let

$$m^1(0) = \max\{m^{\mu}(0) |\ \mu = 1, 2, \ldots, p\}, \qquad [5]$$

The publication costs of this article were defrayed in part by page charge payment. This article must therefore be hereby marked "*advertisement*" in accordance with 18 U.S.C. §1734 solely to indicate this fact.

Abbreviations: HNN and CNN, Hoffmann and conventional neural network models, respectively.

*To whom reprint requests should be addressed.

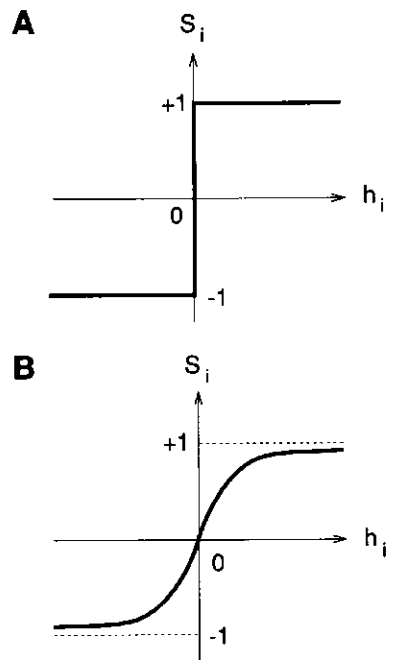

FIG. 1. Input–output response function for the conventional (*A*) discrete (*B*) continuous threshold condition for signalling. S_i, the state of the ith neuron; h_i, the total input signal for the ith neuron.

where

$$m^{\mu}(t) = \frac{1}{N}\,\vec{S}^{\mu}\cdot\vec{S}(t) \qquad [6]$$

is the overlap between the state of the system at time t and the μth pattern. We separate the first term in the total signal (Eq. **1**) into two parts (8).

$$h_i(t) = m^1(t)\,S_i^1 + \frac{1}{N}\sum_{\mu=2}^{p}\sum_{j=1}^{N} S_i^{\mu}\,S_j^{\mu}\,S_j(t); \qquad [7]$$

the first term is proportional to the overlap of the system with pattern $\vec{S}^1$. The second part, the crosstalk term (20), consists of contributions from patterns $\vec{S}^2, \vec{S}^3, \ldots, \vec{S}^p$, which we assume to be Gaussian distributed with an average of zero and a deviation

$$\sigma_{ct} \equiv \sqrt{\frac{p-1}{N}} \qquad [8]$$

in the large N limit (8).

In real physiological and electronic artificial neural systems, the input $h_i(t)$, the state variable $S_i(t)$, the half-width of the bistable region α, and the noise η_i as well as its deviation σ_o are all electric voltages. In the present model, these quantities are shifted and rescaled so that the ground state and the excited state of a neuron are described by $S_i(t) = -1$ and $S_i(t) = +1$, respectively. In such a unit, the maximum input signal is on the order of 1, according to Eq. **7**, whereas the maximum noise level a system without neuronal hysteresis can tolerate is described by a deviation of $\sqrt{2/\pi} \approx 0.8$ (20). The time t is scaled with the average length of an updating cycle.

It follows from Eqs. **4**, **6**, and **7** that

$$m(t+1) = \frac{1}{N}\sum_{i=1}^{N} S_i\,\mathrm{sign}[m(t)S_i + \alpha S_i(t) + \eta'], \qquad [9]$$

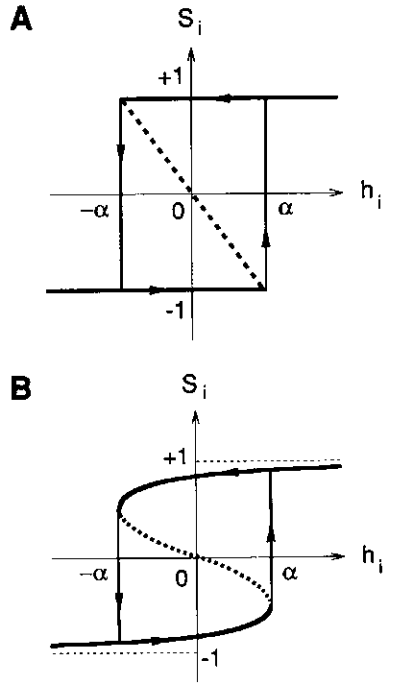

FIG. 2. Input–output response function for a single neuron with hysteresis (*A*) discrete (*B*) continuous threshold condition for signalling. Dashed portions are unstable. S_i, the state of the ith neuron; h_i, the total input signal for the ith neuron.

where η' is the combination of the internal noise η_i and the crosstalk (20). The total SD (20) is

$$\sigma = \sqrt{\sigma_{ct}^2 + \sigma_o^2}. \qquad [10]$$

We have omitted superscript 1 in Eq. **9**; we refer to the overlap between the state of the system with pattern $\vec{S}^1$, unless otherwise specified. Considering the fact that η' is a Gaussian distribution and the value of S_i is either -1 or $+1$, we write the statistical average (8, 20) of Eq. **9** as follows:

$$\langle m(t+1)\rangle = \frac{1}{N}\sum_{i=1}^{N}\{1 - 2\psi[m(t) + \alpha S_i(t)S_i]\}, \qquad [11]$$

with

$$\psi(y) = \frac{1}{\sqrt{2\pi}}\int_{y/\sigma}^{+\infty} e^{-x^2/2}dx. \qquad [12]$$

Suppose that the Hamming distance between the state of the system at time t and the stored pattern is $d(t)$ [$d(t)$ bits different], which is related to the overlap

$$\frac{d(t)}{N} = \frac{1 - m(t)}{2}. \qquad [13]$$

Separating the summation in Eq. **11** in two groups with (*i*) $S_i(t) = S_i$ and (*ii*) $S_i(t) \neq S_i$ or $S_i(t) = -S_i$, and using Eq. **13**, we obtain the *dynamical equation* for the present model

$$\langle m(t+1)\rangle = 1 - \{[1 + m(t)]\,\psi[m(t) + \alpha] + [1 - m(t)]\,\psi[m(t) - \alpha]\}, \qquad [14]$$

which has to be solved iteratively.

The final overlap (the fixed point) is obtained by letting $\langle m(t+1)\rangle = \langle m(t)\rangle \equiv \langle m(\infty)\rangle$ in Eq. **14**. The solutions of $\langle m(\infty)\rangle$ as a function of the noise level σ are obtained by numerical solution of Eq. **14** and presented in Fig. 3, which shows that

the final average overlap $\langle m(\infty)\rangle$ at a given noise level, as well as the critical noise threshold σ_c above which $\langle m(\infty)\rangle$ vanishes, are improved by a nonzero width of the bistable region.

The dynamics of the system given by Eq. **14** show some interesting properties at various noise levels. In Fig. 4 *A–D*, we plot the overlap of the state of the system with pattern $\vec{S}^1$ $\langle m(t)\rangle$, as functions of time t, with initial condition $m(0) = 0$. Fig. 4*A* indicates that at low noise levels the neuronal hysteresis decreases the speed of convergence towards the stored pattern. However, as the noise level increases, the speed of convergence for $\alpha > 0$ gradually surpasses that for $\alpha = 0$, as shown in Fig. 4 *B* and *C*. Fig. 4*D* shows that at high noise levels the convergence rate increases as α increases.

Furthermore, the memory capacity of the network is improved by the neuronal hysteresis. The maximum number of patterns that can be stored in an N-neuron network, $p_{max}(N)$, can be obtained as follows. In the absence of internal noise, i.e., $\sigma_0 = 0$, we have, according to Eqs. **8** and **10**

$$\sigma = \sigma_{cf} = \sqrt{\frac{p-1}{N}}. \qquad [15]$$

The memory of the network reaches its limit if

$$\sqrt{\frac{p_{max}(N)-1}{N}} = \sigma_c, \qquad [16]$$

where the noise threshold σ_c increases with the width of the bistable region, and hence so does $p_{max}(N)$.

Hence we conclude that the overall retrieval ability in the presence of noise and the memory capacity of the present model of neural network are better than in the conventional model.

The physical reason underlying these changes in the present model is the increased tendency of each neuron to remain in its current state (see Eqs. **3** and **4**). This tendency helps the neurons to resist random signals and therefore avoid random neuronal response. The neuronal hysteresis shown in Fig. 2*A* essentially introduces a dead-region centered at zero, which is particularly efficient in suppressing Gaussian-like noises with distributions also centered at zero. These facts also explain the increase of effectiveness in convergence of the system towards the memorized pattern at higher noise levels.

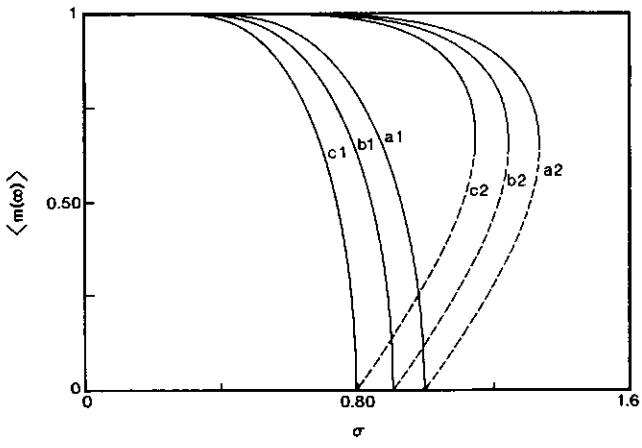

FIG. 3. Plot of average final overlap $\langle m(t=\infty)\rangle$ given by Eq. **14** vs. SD of the Gaussian noise σ for various widths α of the bistable region shown in Fig. 2*A*. For curves a, $\alpha = 0.3$, for curves b, $\alpha = 0.15$, and for curves c, $\alpha = 0$ (the conventional curve). The numerals denote the first order ($\gamma_1 = 1$, $\gamma_2 = 0$, Eq. **14**) (numeral 1) and the second order ($\gamma_1 = \gamma_2 = 1$, Eq. **20**) curves (numeral 2), respectively. Here γ_1 and γ_2 represent the relative strengths of the first- and the second-order interactions, respectively. The dashed portions in the second-order curves are unstable.

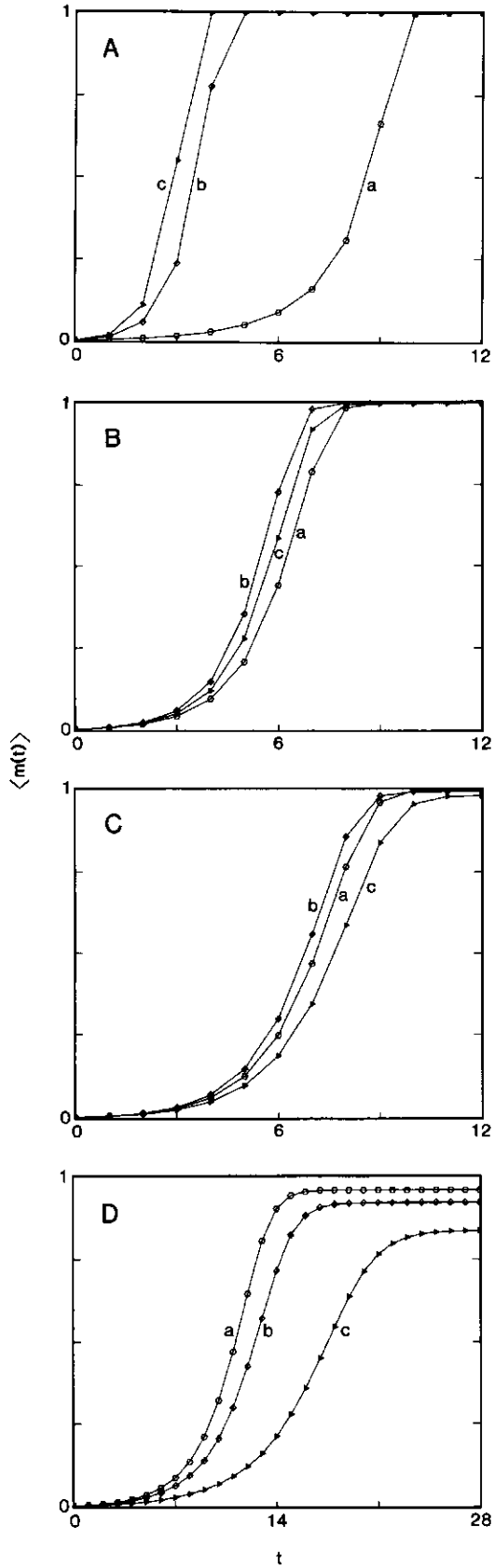

FIG. 4. Plot of average overlap $\langle m(t)\rangle$ given by Eq. **14** as function of time t at different noise levels. In curves a, $\alpha = 0.3$ (○); in curves b, $\alpha = 0.15$ (◇), and in curves c, $\alpha = 0$ (△). R_α denotes the rate of convergence towards the stored pattern when the half-width of the bistable region is α. (*A*) $\sigma = 0.15$, and $R_0 > R_{0.15} > R_{0.3}$. (*B*) $\sigma = 0.34$, and $R_{0.15} > R_0 > R_{0.3}$. (*C*) $\sigma = 0.42$, and $R_{0.15} > R_{0.3} > R_0$. (*D*) $\sigma = 0.6$, and $R_{0.3} > R_{0.15} > R_0$.

However, at low noise levels, the tendency to remain in the current state delays updating and decreases the convergence rate.

We can evaluate the noise threshold σ_c explicitly as a function of the width of the bistable region α. Since the stable solution of Eq. **14** can be considered as the intersecting point of the two sides of Eq. **14** when plotted against m, these two curves must be tangent to each other when $\sigma = \sigma_c$ and $m = \langle m(\infty)\rangle = 0$. Explicitly, σ_c is determined by

$$\frac{1}{\sqrt{2\pi}\sigma_c}[2e^{-\alpha^2/2\sigma_c^2} - \psi(\alpha) + \psi(-\alpha)] = 1. \quad [17]$$

When $\alpha = 0$, Eq. **17** gives $\sigma_c|_{\alpha=0} = \sqrt{2/\pi}$, which is the conventional noise threshold. With the help of Eq. **17** it is not difficult to prove that σ_c increases monotonically as α increases.

SECOND-ORDER INTERACTION

We now consider the effects of inclusion of second-order interactions (9, 20). (For experimental evidence of nonlinear, multiplicative neuronal interactions, see, for example, refs. 28–30.) Instead of Eq. **1**, the total input for the ith neuron (9, 20) is now

$$h_i(t) = \gamma_1 \sum_{j=1}^{N} T_{ij}S_j(t) + \gamma_2 \sum_{j,k=1}^{N} T_{ijk}S_j(t)S_k(t) + \eta_i, \quad [18]$$

where γ_1 and γ_2 measure the relative strengths of the first-order and second-order interactions and

$$T_{ijk} = \frac{1}{N^2}\sum_{\mu-1}^{p} S_i^\mu S_j^\mu S_k^\mu. \quad [19]$$

Instead of Eq. **14** the dynamical equation is now

$$\langle m(t+1)\rangle = 1 - ([1 + m(t)]\,\psi\{\gamma_1 m(t) + \gamma_2[m(t)]^2 + \alpha\} + [1 - m(t)]\,\psi\{\gamma_1 m(t) + \gamma_2[m(t)]^2 - \alpha\}). \quad [20]$$

Compared to the case with only first-order interaction ($\gamma_1 = 1$, $\gamma_2 = 0$), the final retrieval ability is further enhanced by the second-order interaction ($\gamma_1 = 1$, $\gamma_2 > 0$, see Fig. 3). The second-order interaction also causes hysteresis in the retrieval-noise curves (20). We can show analytically that for arbitrary γ_1 and γ_2 (the first and second order) and any given α, the curves $\langle m(\infty)\rangle$ vs. σ always start at $\langle m(\infty)\rangle = 1$, $\sigma = 0$ and end at $\langle m(\infty)\rangle = 0$, $\sigma = \gamma_1\sigma_c$, where σ_c is given by Eq. **17**.

NEUROPHYSIOLOGICAL EVIDENCE FOR HYSTERESIS IN A SINGLE NEURON

Neurons may fire at different rates (number of action potentials per unit time), (see ref. 27, p. 45). This type of neural information transmission is analogous to frequency modulation (FM) in radio broadcasting (27). In the discrete model used in the present discussion, which is also frequently employed in the literature (1–17, 20, 21), a neuron has only two states (on and off, or ± 1), and we assign the on (or $+1$) state to neurons that are firing at a rapid rate and the off (or -1) state to the remainder of the neurons (see ref. 3).

Maintained increases in motoneuronal excitability and prolonged activity resulting from short-lasting synaptic inputs have been reported in the decerebrate cat (31–34). This excitability increase, which outlasts the excitory stimulus train, can stay constant during long periods (even minutes) until it is terminated by an inhibitory impulse train (off stimulus). This behavior supports the present model of neuronal response (see Fig. 2*A* and Eq. **3**): a neuron stays on even after the input falls below the initial firing threshold, until it is turned off by inhibitory input. Experiments (32–34) have shown that this excitability increase is due to an all-or-none plateau depolarization, which is "an intrinsic bistable membrane property"; however, a detailed mechanism needs yet to be developed.

Similar prolonged bursting has been observed in the red nucleus of the turtle cerebellum (35), but further experiments are needed to determine whether it is due to membrane properties of a single neuron or connectivity among neurons (for experimental evidence of hysteresis in squid nerves with clamped electric current, see ref. 36).

Hysteresis in the response of a single neuron presented in Fig. 2 can be interpreted as follows: neurons that have just fired repetitively (been on) have higher excitability compared with neurons that have been quiescent (off). This equivalent interpretation of neuronal hysteresis is helpful in understanding why the following facts support the present view of neuronal response.

Some chemicals show voltage-dependent interactions with sodium channels that produce action potentials: they only increase the excitability of firing neurons and have no effects on quiescent neurons. Hence the presence of these chemicals may induce hysteresis in the level of a single neuron. For instance, batrachotoxin has a strong depolarizing effect on the innervated membrane of the monocellular electroplax preparation from the electric eel while the cell is subject to repetitive stimulation at a stimulus voltage slightly above the threshold for action potential firing (37), whereas no effect on the excitability is observed when the toxin is applied to a resting membrane for a long period of time (up to an hour).

As frequently seen at the neuromuscular junction or at autonomic ganglia, the neuronal excitability can be increased through repetitive stimulation. This phenomenon is well known and often referred to as long-term potentiation (LTP) or posttetanic potentiation (see p. 76 in ref. 27). Although this type of phenomenon occurs on a time scale of seconds and firings of action potentials occur on a time scale of tens of miniseconds, its existence supports the view of neuronal response with hysteresis in the sense that neuronal excitability does depend on the firing *history* of a neuron and neurons that have fired more frequently show higher excitability.

IMPLEMENTATIONS OF THE PRESENT NEURAL NETWORK MODEL

Models of neural networks have been implemented through various physical devices (11–17). An artificial neuron usually consists of an input device, a threshold element, and an output device. For instance, in implementations involving optical devices, the action potentials are represented by laser beams, the synapses are implemented by memory masks (13–16) and holographic elements (17), whereas dynamical updating is performed through feedback loops. The nonlinear electronic and optical devices used so far as threshold elements show no hysteresis in the input–output response function (11–17).

The validity of the predictions on effects of neuronal hysteresis can be readily checked out by carrying out measurements on retrieval performance using an artificial implementation of the present neural network model under different noise levels. There are many nonlinear bistable systems with hysteresis in their input–output relationships, which can be used as thresholding elements in various implementations: chemical (38–41), electronic (42), and optical (for recent review on optical bistability, see refs. 43; 44–46) systems. For instance, optical implementations of the present neural network model can be achieved by replacing the thresholding devices in refs. 13–16 by ZnSe interference filters (44, 45). A variable noise can be easily added to the laser system. The width dependences of retrieval abilities can be evaluated by varying the angle between the surface of the filter and the

incident laser beam because the width of the bistable region in a ZnSe interference filter depends on this angle (44, 45).

COMMENTS

Hoffmann and coworkers have proposed an interesting neural network model (HNN) based on an analogy with the immune system (18, 19). The constituents of the immune system are primarily millions of different clones of lymphocytes. All the cells belonging to one clone are descendants of one cell. Each clone stimulates or suppresses a fraction of other clones. The mathematical model of the system (18, 19) consists of coupled differential equations [see Eq. 7 in ref. 18] on the rate of change $\dot{x}(t)$ of the number of cells in the ith clone according to its dependences on the rate at which it is stimulated and/or killed by a small set of the other cells, which is proportional to

$$y_i(t) = \sum \beta_{ij} x_j(t),$$

with β_{ij} being the interaction matrix between clones, together with a rate of influx of the cells into the system, and a rate of cell death. The nonlinearity in these differential equations gives rise to a hysteresis in the $x_i(t)-y_i(t)$ relation; no direct experimental evidence for the existence of such a hysteresis was presented (18, 19). Hoffmann has made an analogy (18) between $\{x_i(t), y_i(t)\}$ and $\{S_i(t), h_i(t)\}$ in conventional neural network models (CNN) (1–17, 20, 21). There are at least three major differences between the HNN and CNN models. (*i*) There is no Hebbian synaptic plasticity in the HNN; instead, "learning would correspond to the system finding its way (or being led) to a region in the phase space with desired stimulus–response characteristics" (18, 19). (*ii*) There is no upper limit for $x_i(t)$ in the $x_i(t)-y_i(t)$ relationship. In other words, there are no all-or-none thresholding processes, whereas an all-or-none law is present in CNN models where the state variable $S_i(t)$ is bound by its upper (on) and lower (off) limits and in real neurons (see, for example, ref. 27, p. 42). (*iii*) for $N > 2$, the complexity of the differential equations of HNN makes further analytical discussions, such as the dynamics and influence of noise, in the model difficult.

Hoffmann argues that there exist almost 2^N attractors in the neural network model proposed in ref. 18. This is the number of attractors for no or weak correlations between neurons, but the number of attractors may decrease as the correlations between neurons increase. Once the response relation of a single neuron is given, the equilibrium properties, such as the number and locations of attractors, of the network are solely determined by the connectivity—i.e., the interaction matrix. For instance, when the neurons interact strongly only with their nearest neighbors and the interactions are all positive, the network has only two stable states, the all-on state and the all-off state, which are analogous to ferromagnetic states (47). Intermediate cases are analogous to those of spin-glasses (for review, see ref. 48). Gardner has shown that the number of attractors of a CNN can be much larger than N, but this does not increase the information content of the network (49). For a conventional synchronous neural network that consists of N two-state neurons, one can construct, at most, N linearly independent patterns, which determine the maximum information capacity of the network. Personnaz *et al.* (50) have described a pseudo-inverse method that enables one to store an arbitrary set of linearly independent patterns; however, this prescription is rather complex and is difficult to analyze and implement. The widely used Hebbian rule (7, 23) given by Eq. 2 is very cost-effective for being simple and yet having a relatively large information content. In the present discussions, we have adopted the Hebbian rule and have treated correlations between neurons in an approximate fashion—i.e., by assuming the crosstalks (the last term in Eq. 7) to be random and Gaussian distributed (8, 20).

We thank Dr. Geoffrey W. Hoffmann for reading and commenting on the manuscript. We benefited from discussions with Drs. Frank Buchholtz, Yu Chen, Albrecht Freund, Robert Harding, and James Keeler. This work was supported, in part, by the National Science Foundation.

1. Domany, E. (1988) *J. Stat. Phys.* **51,** 743–775.
2. Crick, F. (1989) *Nature (London)* **337,** 129–132.
3. Sompolinsky, H. (1988) *Phys. Today* **41,** 70–80.
4. Little, W. A. (1974) *Math. Biosci.* **19,** 101–120.
5. Hopfield, J. J. (1982) *Proc. Natl. Acad. Sci. USA* **79,** 2554–2558.
6. Hopfield, J. J. (1984) *Proc. Natl. Acad. Sci. USA* **81,** 3088–3092.
7. Cooper, L. N., Liberman, F. & Oja, E. (1979) *Biol. Cybern.* **33,** 9–28.
8. Kinzel, W. (1985) *Z. Phys.* **B60,** 205–213.
9. Peretto, P. & Niez, J. J. (1986) *Biol. Cybern.* **54,** 53–63.
10. Crick, F. & Asanuma, C. (1986) in *Parallel Distributed Processing*, eds. McClell, J. L. & Rumelhart, D. E. (MIT Press, Cambridge, MA) Vol. 2, pp. 333–371.
11. Jackel, L. D., Howard, R. E., Graf, H. P., Straughn, B. & Denker, J. S. (1986) *J. Vac. Sci. Technol.* **B4,** 61–63.
12. Agranat, A. & Yariv, A. (1987) *Electronics Lett.* **23,** 580–581.
13. Farhat, N. H., Psaltis, D., Prata, A. & Paek, E. (1985) *Appl. Opt.* **24,** 1469–1475.
14. Psaltis, D. & Farhat, N. H. (1985) *Opt. Lett.* **10,** 98–100.
15. Psaltis, D., Park, C. H. & Hong, J. (1988) *Neural Networks* **1,** 149.
16. Ohta, J., Tai, S., Oita, M., Kuroda, K., Kyuma, K. & Hamanaka, K. (1989) *Appl. Opt.* **28,** 2426–2428.
17. Anderson, D. Z. & Erie, M. C. (1987) *Opt. Eng.* **26,** 434–444.
18. Hoffmann, G. W. (1986) *J. Theor. Biol.* **122,** 33–67.
19. Hoffmann, G. W., Benson, M. W., Bree, G. M. & Kinahan, P. E. (1986) *Physica* **22D,** 233–246.
20. Keeler, J. D., Pichler, E. E. & Ross, J. (1989) *Proc. Natl. Acad. Sci. USA* **86,** 1712–1716.
21. Peretto, P. (1984) *Biol. Cybern.* **50,** 51–62.
22. McCulloch, W. S. & Pitts, W. (1943) *Bull. Math. Biophys.* **5,** 115–133.
23. Hebb, D. O. (1949) *The Organization of Behavior* (Wiley, New York), p. 44.
24. Shaw, G. L. & Vasudevan, R. (1974) *Math. Biosci.* **21,** 207–218.
25. Sejnokwski, T. J. (1981) in *Parallel Models of Associative Memory*, eds. Hinton, G. & Anderson, J. (Lowrence Erlbaum, Hillsdale, NJ) pp. 189–212.
26. Abeles, M. (1982) *Local Cortical Circuits* (Springer, New York).
27. Carpenter, R. H. S. (1984) *Neurophysiology* (University Park Press, Baltimore, MD).
28. Kandel, E. R. & Tauc, L. (1965) *J. Physiol.* **181,** 1–27.
29. Roney, K. J., Scheibel, A. B. & Shaw, G. L. (1979) *Brain Res. Rev.* **1,** 225–271.
30. Shaw, G. L., Harth, E. & Scheibel, A. B. (1982) *Exp. Neurol.* **77,** 324–358.
31. Hultborn, H., Wigström, H. & Wängberg, B. (1975) *Neuro-Sci. Lett.* **1,** 147–152.
32. Hounsgaard, J., Hultborn, H., Jespersen, B. & Kiehn, O. (1984) *Exp. Brain Res.* **55,** 391–394.
33. Crone, C., Hultborn, H., Kiehn, O., Mazieres, L. & Wigström, H. (1988) *J. Physiol. (London)* **405,** 321–343.
34. Hounsgaard, J., Hultborn, H., Jespersen, B. & Kiehn, O. (1988) *J. Physiol. (London)* **405,** 345–367.
35. Keifer, J. & Houk, J. C. (1989) *Neuro-Sci. Lett.* **97,** 123–128.
36. Guttman, R., Lewis, S. & Rinzel, J. (1980) *J. Physiol.* **305,** 377–395.
37. Bartels-Bernal, E., Rosenberry, T. L. & Daly, J. W. (1977) *Proc. Natl. Acad. Sci. USA* **74,** 951–955.
38. Creel, C. L. & Ross, J. (1976) *J. Chem. Phys.* **65,** 3779–3789.
39. Zimmermann, E. C., Schell, M. & Ross, J. (1984) *J. Chem. Phys.* **81,** 1327–1336.
40. Ross, J. (1985) *Ber. Bunsenges. Phys. Chem.* **89,** 605–619.
41. Kramer, J. & Ross, J. (1985) *J. Chem. Phys.* **83,** 6234–6241.
42. Pasmanter, R. A., Bedeaus, D. & Mazur, P. (1978) *Physica* **90A,** 151–163.
43. Daunois, A. & Bigot, J. Y. (1988) *Appl. Phys.* **B45,** 157–162.
44. Smith, S. D., Mathew, J. G. H., Taghizadeh, M. R., Walker, A. C., Wherrett, B. S. & Hendry, A. (1984) *Opt. Commun.* **51,** 357–362.
45. Kim, B. G., Garmire, E., Shibata, N. & Zembutsu, S. (1987) *Appl. Phys. Lett.* **51,** 475–477.
46. Frank, D. & Wherrett, B. S. (1987) *Op. Eng.* **26,** 53–59.
47. Callaway, J. (1974) *Quantum Theory of the Solid State* (Academic, New York).
48. Binder, K. & Young, A. P. (1986) *Rev. Mod. Phys.* **58,** 801–965.
49. Gardner, E. (1987) *Europhys. Lett.* **4,** 481–485.
50. Personnaz, L., Guyon, I. & Dreyfus, G. (1985) *J. Phys. Lett. (Paris)* **46,** L359–L365.